where $\omega^i = \partial\xi^i/\partial t$. Substituting B^α in Eqs. (10) and (11) into Eq. (8), we obtain the expression in its usual form

$$\frac{\partial}{\partial t}(JA) + \frac{\partial}{\partial \xi^i}[J(f^i + A\omega^i)] = JC \tag{12}$$

or, in terms of Cartesian components,

$$\frac{\partial}{\partial t}(JA) + \frac{\partial}{\partial \xi^i}\left[J\left(f_c^j \frac{\partial \xi^i}{\partial x^j} + A\omega^i\right)\right] = JC \tag{13}$$

If A, C, and f^j are also vectors in L^3, by equating the components of E_i^c in Eq. (13), the scalar form may be obtained

$$\frac{\partial}{\partial t}(JA_c^k) + \frac{\partial}{\partial \xi^i}\left[J\left(f_{cc}^{jk} \frac{\partial \xi^i}{\partial x^j} + A_c^k\omega^i\right)\right] = JC_c^k \tag{14}$$

For a steady coordinate system ω^i vanishes.

Numerical Considerations

For numerical purposes, the terms $\partial\xi^\alpha/\partial x^\beta$ may be evaluated in terms of $\partial x^\alpha/\partial\xi^\beta$ from the following expression:

$$\frac{\partial \xi^\alpha}{\partial x^\beta} = \frac{R_{\alpha\beta}}{J} \tag{15}$$

Here $R_{\alpha\beta}$ are the algebraic complements of the Jacobian matrix $\partial x^\alpha/\partial\xi^\beta$.

On the other hand, the geometric conservation law[6] may also be obtained in a more direct and simpler fashion. It is noted that Eq. (2) is satisfied for any constants A, f, and zero C concurrently with Eq. (8), which gives

$$\frac{\partial}{\partial \xi^\alpha}\left(J\frac{\partial \xi^\alpha}{\partial x^\beta}\right) = \frac{\partial R_{\alpha\beta}}{\partial \xi^\alpha} = 0, \qquad \beta = 1,2,3,4 \tag{16}$$

In particular, $\beta = 4$ results in the geometric conservation law. Hence the necessary requirement of a conservative discrete operator that approximates Eq. (13) or (14) is such that Eq. (16) should be satisfied.

It is sufficient to mention here that the correct conservation forms of diverse fluid dynamic equations (e.g., the Navier-Stokes equations) can be obtained by selecting appropriate quantities for A, f, and C. For the case of two-dimensional equations, i, j, and k should denote the components in L^2 and α and β in L^3. Here, of course, the third added base vector denotes time t.

Concluding Remarks

A more direct method than has been reported previously to derive the conservative form of the equations of fluid dynamics in general nonsteady curvilinear coordinates has been presented. The geometric conservation law has also been derived as an aid to the development of compatible numerical algorithms.

Acknowledgment

This research was supported by the National Sciences and Engineering Research Council of Canada under Grant CNR-A8846.

References

[1]McVittie, G. C., "A Systematic Treatment of Moving Axes in Hydrodynamics," *Proceedings of the Royal Society, Ser. A*, Vol. 196, No. A1044, Feb. 1949, pp. 285-300.

[2]Viviand, H., "Formes conservatives des équations de la dynamique des gaz," *La Recherche Aérospatiale,* Année 1974, No. 1, Jan.-Feb. 1974, pp. 65-66.

[3]Daubert, A. and Graffe, O., "Quelques aspects des écoulements presque horizontaux a deux dimensions en plan et non-permaments application aux estuaires," *La Houille Blanche*, Vol. 8, 1967, pp. 847-860.

[4]Vinokur, M., "Conservation Equations of Gas Dynamics in Curvilinear Coordinate Systems," *Journal of Computational Physics*, Vol. 14, Feb. 1974, pp. 105-125.

[5]Warsi, Z. U. A., "Conservation Form of the Navier-Stokes Equations in General Nonsteady Coordinates," *AIAA Journal*, Vol. 19, Feb. 1981, pp. 240-242.

[6]Thomas, P. D. and Lombard, C. K., "The Geometric Conservation Law—A Link between Finite-Difference and Finite-Volume Methods of Flow Computation on Moving Grids," AIAA Paper 78-1208, July 1978.

Finite Difference Solutions of the Euler Equations in the Vicinity of Sharp Edges

P.-M. Hartwich*
NASA Langley Research Center, Hampton, Virginia

Introduction

NUMEROUS attempts have been made to explain why finite difference solutions of the Euler equations can describe flows with large vortical structures around sharp-edged bodies. Some investigators[1,2] claim compressibility effects are the underlying mechanism for the generation of the necessary vorticity, others[3,4] suspect that artificial numerical damping is the causative agent.

The basic idea of the present approach is to study the influence of a singular sharp edge on the truncation error for a set of discretized Euler equations. First, the distribution of the truncation error of one finite difference approximation of the Euler equations near a sharp edge of a thin plate is analyzed. This leads to a determination of the size of the region of the neighborhood of such a singularity, where the leading terms of the truncation error are of the same order as the terms describing the changes in momentum and pressure. Finally, these results are verified in numerical experiments.

Consistency of a Discretization of the Euler Equations

The Euler equations in nondivergence formulation for an incompressible flow are written in nondimensional variables as

$$\frac{\mathrm{D}v}{\mathrm{D}t} = -\nabla p \tag{1}$$

with $v = (u'/v_\infty, v'/v_\infty, 0)$ and $p = p'/(\rho v_\infty^2)$. These equations are discretized explicitly with respect to time and with centered space difference quotients representing the spatial derivatives. They are solved by using a time-marching technique that will be described more in detail in the next section. Such a discretization of the Euler equations is unconditionally unstable unless numerical damping is added. For this reason, a generalized Lax method[4,5] is employed. The result-

Received Dec. 10, 1984; revision received Jan. 2, 1985.

*National Research Council Associate.

ing finite difference approximation of the x momentum equation is

$$\{u_{i,j}^{m+1} - [1-2(\phi_1+\phi_2)_{i,j}^m]u_{i,j}^m - \phi_{1,i,j}^{\;m}(u_{i+1}+u_{i-1})_j^m$$
$$-\phi_{2,i,j}^{\;m}(u_{j+1}+u_{j-1})_i^m\}/\Delta t + u_{i,j}^m(u_{i+1}-u_{i-1})_j^m/2h$$
$$+(v_{i,j}^m(u_{j+1}-u_{j-1})_i^m/2h = (p_{i+\frac{1}{2}}-p_{i-\frac{1}{2}})_j/h \quad (2)$$

where

$$\phi_{k,i,j}^{\;m} = [u_{k,i,j}^{\;m}(\Delta t/h)]^2/2, \; k=1,2 \quad (3)$$

The subscripts i and j refer to the location of the grid points in the x and y directions, respectively. Similarly, the time level is denoted by the superscript m. Note also that a uniform spatial step size is being used, that is, $\Delta x = \Delta y = h = \text{const}$. Unlike the original Lax method[6] (i.e., $\phi_k = \text{const} = 0.5$), the finite difference formulation of Eq. (2) is unconditionally consistent with the corresponding differential equation, under the assumption that the truncation error can be controlled by the time and spatial step sizes. Dropping the subscripts for clarity, the leading terms of the truncation error are

$$\epsilon_1 = \frac{\Delta t}{2}\frac{\partial^2 u}{\partial t^2} + \frac{h^2\Phi_1}{\Delta t}\frac{\partial^2 u}{\partial x^2} + \frac{h^2\Phi_2}{\Delta t}\frac{\partial^2 u}{\partial y^2}$$
$$-\frac{h^2 u}{6}\frac{\partial^3 u}{\partial x^3} - \frac{h^2 v}{6}\frac{\partial^3 u}{\partial y^3} - \frac{h^2}{24}\frac{\partial^3 p}{\partial x^3} \quad (4)$$

The discretization of the momentum equation in y direction and the corresponding truncation error can be formulated[5] in a fashion similar to Eqs. (2) and (4).

Assuming the finite difference solution has reached an asymptotic steady state, the derivative of the pressure can be replaced by gradients of the velocities by differentiating the x momentum equation twice with respect to x. The derivatives of second- and third-order act like diffusion and dispersion of momentum, respectively. The truncation error ϵ, therefore, is split into two parts. Using Eq. (3), one obtains

$$\epsilon_1 = \frac{h^2}{\Delta t}\left(\Phi_1\frac{\partial^2 u}{\partial x^2} + \Phi_2\frac{\partial^2 u}{\partial y^2}\right) = \Delta t\left(\frac{u^2}{2}\frac{\partial^2 u}{\partial x^2} + \frac{v^2}{2}\frac{\partial^2 u}{\partial y^2}\right) \quad (5)$$

$$\epsilon_2 = h^2\left\{\frac{1}{8}\frac{\partial u}{\partial x}\frac{\partial^2 u}{\partial x^2} - \frac{v}{6}\frac{\partial^3 u}{\partial y^3}\right.$$
$$\left.-\frac{1}{24}\left[3u\frac{\partial^3 u}{\partial x^3} - \frac{\partial^2}{\partial x^2}\left(v\frac{\partial u}{\partial x}\right)\right]\right\} \quad (6)$$

The influence of numerical damping is reflected by ϵ_1 and the dispersion of momentum is described by ϵ_2.

Now, consider a steady, incompressible, irrotational, and attached flow around a sharp-edged, semi-infinite plate of zero thickness. For Cartesian coordinates, the flowfield is described by a potential flow solution,[7]

$$\psi(x,y) = 2(x^2+y^2)^{1/4}\sin\{\tfrac{1}{2}[\text{arctg}(y/x)]\} \quad (7)$$

At the edge, the velocity components and all their derivatives are infinite. If the edge and a small neighboring region are excluded from a finite difference solution of the Euler equations, then it is expected that their numerical solution approximates the potential flow solution, since the velocity distribution is smooth and the truncation errors are controllable by the time and spatial step sizes. In order to estimate the size of that region, the truncation errors [Eqs. (5) and (6)] are evaluated by the potential flow solution [Eq. (7)]. Figure 1 shows the distribution of the normalized truncation errors $|\epsilon_1|/\Delta t$ and $|\epsilon_2|/h^2$. To simplify the discussion of the numerical results given below, the values of the time step Δt and the square of the spatial step h^2 were taken to be the same; that is, $\Delta t = h^2$. A common value of 10^{-2} was used in the current work. Thus, the region that must be excluded from this finite difference solution is described by the union of the areas that are enclosed by the contours $|\epsilon_1|/\Delta t = 1$ and $|\epsilon_2|/h^2 = 1$. If this region is not excluded, one can no longer be sure whether one really obtains an approximate solution to the Euler equations or a solution to some difference equations that contain terms looking like the ones which act as friction forces in the Navier-Stokes equations or which act like dispersion in equations that describe the propagation of waves.

Numerical Experiments

The results obtained from the analytical investigations are applied to a finite difference solution of the Euler equations for an incompressible, steady, and planar flow around a finite plate of zero thickness, positioned perpendicularly to the freestream. In Fig. 2, five boundaries (I-V) are indicated. The boundary conditions along boundaries I-IV are:

$$\text{I)}: \; u=1, \; \frac{\partial v}{\partial x}=0 \qquad \text{II)}: \; v=\frac{\partial u}{\partial y}=0$$

$$\text{III)}: \; \frac{\partial v}{\partial x}=\frac{\partial^2 u}{\partial x^2}=0 \qquad \text{IV)}: \; \frac{\partial u}{\partial y}=\frac{\partial^2 v}{\partial y^2}=0$$

Since a staggered mesh is used, boundary conditions for the pressure are not required. The area encompassed by the line of symmetry (II) and by line V was excluded from the finite difference solution. In this region and along line V, the velocity components were prescribed using the analytical solution for the attached potential flow around a flat plat set

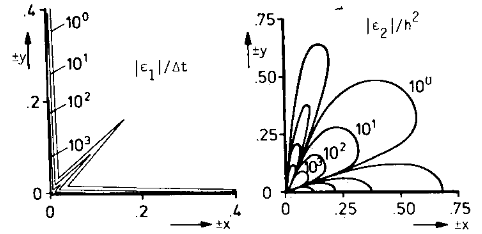

Fig. 1 Distribution of the leading terms of the trucation error of a set of discretized Euler equations around a sharp edge.

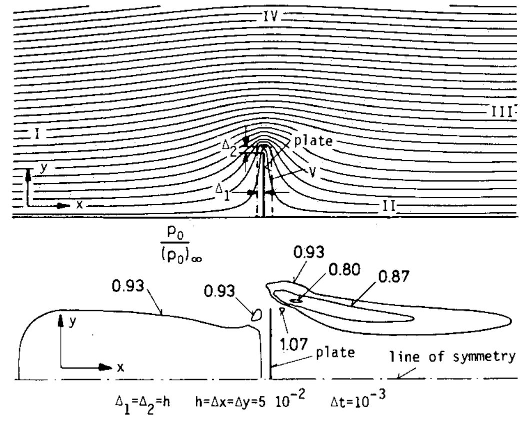

Fig. 2 Finite difference solution of the Euler equations for a flow around a thin plate.

up perpendicular to the freestream,

$$w(z) = u(x,y) + \mathrm{I}v(x,y) = (x + \mathrm{I}y)[a^2 + (x + \mathrm{I}y^2)]^{-1/2} \quad (8)$$

where $\mathrm{I} \equiv \sqrt{-1}$ and a denotes the half-span of the plate. The lengths Δ_1 and Δ_2 determine the size of that region. The finite difference approximations of the momentum equations are formulated analogously to Eq. (2). The pressure and velocity fields are computed simultaneously by iteration. The relationship between pressure and velocity is given by

$$p_{i,j}^{n+1} = p_{i,j}^{n} - \frac{h^2}{8\Delta t}(\nabla_\delta \cdot v)_{i,j}^{n,m+1} \quad (9)$$

where the equation of continuity is used as a condition of compatibility.[4,5] The divergence of v, $\nabla_\delta \cdot v$, is approximated by centered space difference quotients. This iterative procedure is repeated within each time step, until the velocity field is source free, i.e.,

$$\max|\nabla_\delta \cdot v|_{i,j}^{n,m+1} < h^2$$

The solution is assumed to have obtained an asymptotic steady state, if

$$\max\left|\frac{v_{i,j}^{m+1} - v_{i,j}^{m}}{\Delta t}\right| < \Delta t$$

The computational domain consists of 70×30 grid points in x and y directions, respectively. The time step is $\Delta t = 10^{-3}$ and the constant mesh width is $h = 5 \times 10^{-2}$. The size of the region, where the solution is prescribed, is determined by $\Delta_1 = \Delta_2 = h$.

The streamlines in Fig. 2 show a steady-state, finite difference solution of the Euler equations. This solution seems to be reasonable according to the chosen set of boundary conditions. However, the corresponding lines of constant normalized total pressure displayed in Fig. 2 reveal that the flowfield is not only rotational, but also has no physical meaning at all since a zone exists where the total pressure is higher than the freestream value. These computations were repeated with all parameters chosen as in the first case, but with larger values of Δ_1 and Δ_2. The area with the prescribed analytical solution was increased by setting $\Delta_1 = \Delta_2 = 2h$. Using the same set of boundary conditions and values for the parameters Δt and h, a valid finite difference solution of the Euler equation is obtained. The streamline pattern differs only marginally from the one shown in Fig. 2 and no gradients in total pressure can be detected anywhere.

Conclusions

If an inviscid, incompressible and steady flow around a sharp edge is to be obtained by a finite difference solution of the Euler equations, the region around such a singularity must be treated very carefully. The closer the finite difference solution domain approaches that singular point, the more the leading terms of the truncation error, characterized as diffusion and dispersion of momentum, have a tendency to increase in an unbounded fashion. Then the consistency of the discretized Euler equations with their differential formulation is no longer ensured. Consequently, one cannot judge whether an approximate solution of the Euler equation is obtained or a set of difference equations is solved that has nothing in common with the original differential problem. To avoid these difficulties, it is recommended that the region in the immediate vicinity of a singular sharp edge should be excluded from a finite difference solution of the Euler equations. In that region, the solution should be constructed separately. If available, an analytical solution can be useful, as demonstrated in the numerical tests reported above.

References

[1] Rizzi, A., "Damped Euler Equation Method to Compute Transonic Flow Around Wing Body Combinations," *AIAA Journal*, Vol. 20, Oct. 1982, pp. 1321-1328.

[2] Schmidt, W. and Jameson A., "Euler Equations as a Limit of Infinite Reynolds Number for Separation Flows and Flows with Vortices," *Lecture Notes in Physics*, Vol. 170, edited by E. Krause, Springer-Verlag, Berlin, 1982, pp. 468-471.

[3] Rizzi, A., "Influence on Vortex Shedding in Inviscid Flow Computations," *Recent Contributions to Fluid Mechanics*, edited by W. Haase, Springer-Verlag, Berlin, 1982, pp. 213-221.

[4] Krause, E., Shi, X.-G., and Hartwich, P.-M., "Computations of Leading Edge Vortices," AIAA Paper 83-1907.

[5] Hartwich, P.-M., "Berechnung von Vorderkantenwirbeln an Deltafluegln," Doctoral Thesis, Rheinisch-Westfaelische Technische Hochschule Aachen, FRG, 1983.

[6] Lax, P. D., "Weak Solutions of Nonlinear Hyperbolic Equations and Their Numerical Treatment," *Communications on Pure and Applied Mechanics*, Vol. 7, 1954, pp. 159-207.

[7] Schlichting, H. and Truckenbrodt, E., *Aerodynamik des Flugzeuges*, Pt. I, 2nd ed., Springer-Verlag, Berlin, 1967.

Stagnation Point Flows with Freestream Turbulence—The Matching Condition

Warren C. Strahle*

Georgia Institute of Technology, Atlanta, Georgia

Introduction

THE calculation of stagnation point flows with imbedded freestream turbulence is of practical importance in many situations. In particular, the combustor exhaust flow impacting on the nozzle guide vanes in a gas turbine is one example, and the heat transfer at a reattachment point of a separated turbulent flow is another. A difficulty has recently been found, however, in a k-ϵ calculation in attaining a proper match between the outer freestream flow and the turbulent/laminar viscous sublayer. Resolution of this problem for the outer freestream flow is the subject of this Note.

Analysis

It is common practice in eddy viscosity approaches to the calculation of turbulent stagnation point flows to assume that at the outer edge of the viscous layer the turbulence quantities such as k (turbulent kinetic energy) correspond to "freestream" values.[1-3] This presents the first dilemma. Far from a body in high Reynolds number turbulence with no mean velocity gradients (no turbulence production), convection and dissipation should balance each other. Sitting on a fluid particle one merely sees a purely decaying turbulence field as the body is approached. The point here is that there is no unique freestream condition and it is changing constantly along a streamline. The resolution of this conflict is, however, fairly easy. A point or plane in the flowfield must be selected as the appropriate "infinity" and the turbulence specified there. In an experiment it could be just downstream of a physical grid. In a gas turbine combustor it could be the last downstream station at which significant turbulence generation takes place on the stagnating streamline of interest. Specifying

Received Jan. 23, 1985; revision received March 12, 1985.

*Regents Professor, School of Aerospace Engineering. Associate Fellow AIAA.